IEEE Access
Multidisciplinary | Rapid Review | Open Access Journal

Received September 9, 2019, accepted October 12, 2019, date of publication October 17, 2019, date of current version October 31, 2019.

Digital Object Identifier 10.1109/ACCESS.2019.2948107

Heart Rate Tracking Using a Wearable Photoplethysmographic Sensor During Treadmill Exercise

YOUNGSUN KONG AND KI H. CHON, (Senior Member, IEEE)
Department of Biomedical Engineering, University of Connecticut, Storrs, CT 06269, USA

Corresponding author: Ki H. Chon (ki.chon@uconn.edu)

This work was supported in part by the National Institutes of Health (NIH) under Grant 1R01HL137734, and in part by the National Science Foundation (NSF) under Grant 1522087.

ABSTRACT We present a beat-to-beat heart rate tracking algorithm that is designed especially to handle the nonstationary motion artifacts often encountered using photoplethysmographic (PPG) signals acquired from smartwatches or a forehead-worn device, during intense exercise. To date, many algorithms have been based on tracking heart rates during intense exercise using an 8-second average of heart rates, which does not accurately capture the large variation in instantaneous heart rates during exercise. In this paper, we propose a novel technique that can accurately estimate heart rates from wearable PPG signals with subjects running on a treadmill and making other sudden movements. The proposed algorithm includes three parts: 1) time-frequency spectrum estimation of PPG and accelerometer signals, 2) motion artifact removal by subtraction of the time-frequency spectra of the accelerometer signals from the PPG signals, and 3) postprocessing to further reject motion artifact-affected heart rates followed by interpolation of removed heart beats using a cubic spline approach. The proposed approach was compared to one of the recent and most accurate algorithms. The results of the proposed and compared algorithms were evaluated with two datasets (IEEE Signal Processing Cup (N=12) and our own dataset (N=10)) obtained from a smartwatch and a forehead PPG sensor with subjects running on a treadmill. The reference heart rates were obtained from a chest-worn ECG. Our method, using a 12 second windowed segment, resulted in an average absolute error of only 2.94 beats per minute and an average relative error of 2.42 beats per minute, which are a 71% and 94% improvement, respectively, over the compared algorithm.

INDEX TERMS Motion artifact, photoplethysmogram, wearable sensor, heart rate, VFCDM, accelerometer, beat-by-beat heart rate, treadmill.

I. INTRODUCTION

With the rise in popularity of smart wearable devices, heart rates are routinely measured [1]–[3]. Unlike traditional medical devices, smart wearable devices enable monitoring and recording of physiological data anytime and anywhere, and heart rates (HR), activity recognition, and calorie consumption are some of the most popular metrics measured [4]–[6]. The electrocardiogram (ECG) and photoplethysmogram (PPG) are often used to measure HR, with the latter device being the most popular approach with smart wearable devices [7]. Although ECG signals are generally considered the gold standard, their use is limited especially in wearable devices when continuous monitoring is required. Apple Watch Series 4 now contains dry electrodes which allow the recording of 30 seconds of ECG data, albeit mostly for detecting the presence of atrial fibrillation. However, smartwatches now all contain PPG sensors which can be used to make continuous heart rate measurements. A photodiode in a PPG sensor detects the change of blood volume in the microvascular bed of tissue by illuminating the skin with a light-emitting diode (LED). PPG signals can be exploited to extract a plethora of physiological information such as HR, heart rate variability (HRV), respiratory rate, and oxygen saturation [8]–[11]. In addition, many investigators have used PPG data to examine the feasibility of detecting various cardiovascular arrhythmias [12], [13]. For example, the Chon lab developed atrial fibrillation detection algorithms using smartphone and smartwatch PPG signals [13], [14] and other investigators have also used smartwatch PPG signals [15].

The associate editor coordinating the review of this manuscript and approving it for publication was Hasan S. Mir.

However, it is well known that PPG signals obtained from wearable devices are prone to severe motion artifacts (MAs) which prevent reliable estimation of HR. MAs can be due to either repetitive movements or sudden movements, with the former being the easier to filter out as long the repetitive frequency does not coincide with the HR at that time instant.

Many methods have been explored to detect MAs and remove them from PPG signals [16]–[20]. A moving average approach is often employed to remove intermittent noise. More computationally intensive MA removal methods such as adaptive filtering [16], Wiener filtering [17], independent component analysis [18], principal component analysis [19], and Kalman filtering [20] have been used with some success.

Spurred by the advent of smartwatches and the IEEE Signal Processing Challenge Cup competition, several accurate algorithms for heart rate extraction during intense exercise protocols have been developed [21]–[24]. The competition started with the development of the algorithm known as TROIKA, which consists of signal decomposition for denoising, sparse signal reconstruction for high-resolution spectrum estimation, and spectral peak tracking with verification [21]. Since then, many algorithms have been developed to increase HR accuracy, including JOSS. It employs joint sparse spectrum reconstruction using a multiple measurement vector, followed by spectral peak tracking with verification [22]. SpaMA is another algorithm, which showed higher accuracy than either TROIKA or JOSS and is based on reconstructing MA-corrupted PPG signals and finding HR based on time-varying spectral analysis [23]. To date, Temko's method showed one of the highest accuracies by using the Wiener filter to attenuate the MAs and a phase vocoder to refine the HR estimates, with the option of an offline preprocessing method using Viterbi decoding [24]. This method is henceforth referred to as the Wiener filter and phase vocoder (WFPV).

All of the aforementioned and other MA removal algorithms are based on taking 8-second segments of data that are time-shifted every second. Thus, this approach does not provide instantaneous or beat-to-beat heart rate estimation but rather an 8 second average of heart rates, which does not provide an accurate measure of heart rate dynamics, especially when subjects are exercising intensively. To overcome this limitation, we propose a beat-to-beat or instantaneous estimate of heart rate rather than an 8 second averaged heart rate. To this end, our new method is developed to estimate HR from MA-corrupted PPG signals, consisting of 1) time-frequency spectrum (TFS) estimation of PPG signals and accelerometer signals using variable-frequency complex demodulation (VFCDM), which has one of the highest time and frequency resolutions, to estimate HRs and their associated amplitudes [25], 2) MA removal by subtraction of the estimated TFS of accelerometer signals from that of the PPG data, and 3) post-processing to remove remaining noise artifacts and interpolate the missing heart rate data. The results of our method were compared with those of WFPV [24]. Henceforth our method is defined as time-varying spectral motion artifact removal technique (TVSMART).

This paper is organized as follows. The datasets and methods are described in Section II. The results are presented and compared with other methods in Section III, and conclusions are drawn in Section IV.

II. METHODS

A. DATASETS

Our method, TVSMART, was evaluated with two different PPG databases. The first database is from the 2015 IEEE signal processing challenge competition and the data consists of wrist-worn PPG signals during walking and running on a treadmill [26]. The dataset provides reference ECG HRs on a beat-to-beat basis. The second dataset is our own lab's (Chon lab) data and it includes PPG signals from the forehead while subjects were walking and running on a treadmill [23]. The protocols of both datasets are described in Table 1. For our own dataset, we collected beat-to-beat ECG heart rates and these were used as the reference. The objective was to compare estimated HRs with the reference ECG HRs for each beat rather than an 8 second moving average with a 2 second time shift. The reference HR was calculated beat-to-beat from the ECG electrodes placed on the chest. ECG electrodes and leads were secured to the subject's skin with a tape to minimize motion artifacts.

TABLE 1. Datasets.

Index	Dataset	Activity Type	Age and Sex	Remarks
1	IEEE Cup	Type 1	13-38 Male	Wrist Green LED (609 nm)
2				
3				
4				
5				
6				
7				
8				
9				
10				
11				
12				
13	Chon Lab Data	Type 2	26-55 9 Male, 1 Female	Forehead Red & Infrared LED (660 and 940 nm)
14				
15				
16				
17				
18				
19				
20				
21				
22				

Type 1 (IEEE Cup Data)						
Seconds	30	60	60	60	60	30
Speed (km/h)	1-2	6-8	12-15	6-8	12-15	1-2

Type 2 (Chon Lab Data)								
Seconds	60	60-150	60	120-150	60	60-150	60	60
Speed (km/h)	0	4.8	0	8	0	11.3	0	A

* A: Arbitrary movement

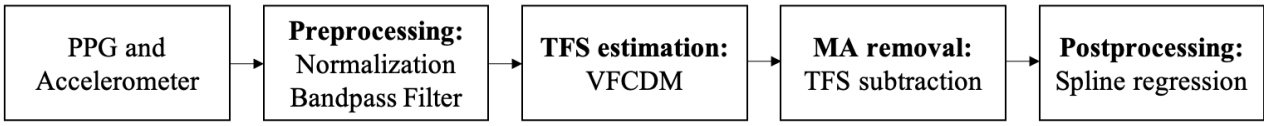

FIGURE 1. Flowchart of the proposed HR tracking method.

1) IEEE CUP

PPG signals were recorded from the wrist using a 2 channel pulse oximeter with a green LED. Triaxial acceleration data were also recorded from the same PPG sensor's wrist band. The ECG signals were recorded from the chest as the reference HR. All signals were sampled at 125 Hz. All data were recorded on a treadmill with various speeds ranging from 1 to 15 km/h.

2) CHON LAB

A forehead PPG sensor developed in our lab was used to record signals using both infrared and red LEDs. Triaxial acceleration data were simultaneously recorded from the same forehead PPG sensor. Both accelerometer and PPG data were collected at 100 Hz. The reference ECG signals were simultaneously collected from a Holter monitor with a sampling frequency of 400 Hz. All data were recorded with subjects on a treadmill with various speeds ranging from 3 to 7 miles/h. In the last minute, data was taken while the subjects made arbitrary arm and head movements while being otherwise stationary.

B. HR ESTIMATION

Figure 1 shows a flowchart of our HR tracking method. Our method consists of the following sequential steps: preprocessing using normalization, bandpass filtering, TFS estimation and MA removal using the VFCDM approach, and estimation of HRs using cubic spline regression. Each of these sequential steps are described below.

1) PREPROCESSING

Data are processed in two ways. First, for post-processing of the entire dataset, all PPG signals and accelerometer signals are resampled to 20 Hz. Second, for a windowed data approach, all PPG signals and accelerometer signals are segmented with a 12-second window which is then shifted every 4 seconds; these segments are then resampled to 20 Hz. The PPG signals and tri-axial accelerometer signals for both the entire dataset and each windowed segment are then filtered with a 5^{th} order Butterworth bandpass and highpass filter, (0.9 Hz – 3.2 Hz and a cutoff frequency of 0.5 Hz) since the HR range in this study is presumed to be between 55-190 beats/min even when accounting for HRs during intense exercise. PPG signals for both the entire dataset and the 12-sec windowed segments are normalized to zero mean and unit variance, and then averaged as follows:

$$PPG = \sum_{i=1}^{n} \frac{(ppg_i - \mu_i)/\sigma_i}{n},$$

where n represents the number of PPG channels. Also, each accelerometer signal is normalized to zero mean and unit variance.

2) VFCDM

The VFCDM-based time-frequency spectrum is chosen to obtain the TFS of PPG and accelerometer signals to remove MAs and extract HR. VFCDM has been shown to exhibit one of the highest time and frequency spectral resolutions while retaining accurate amplitude estimates when compared to other methods such as the smooth pseudo Wigner-Ville and continuous wavelet transform. Since details of the VFCDM are described in [25], we briefly summarize the VFCDM algorithm in this section. A sinusoidal signal x(t) is considered to be a narrow band oscillation with a center frequency f_0, instantaneous amplitude A(t), phase $\phi(t)$, and the direct current component dc(t), as follows:

$$x(t) = dc(t) + Acos(2\pi f_0 t + \phi(t)) \tag{1}$$

For a given center frequency, the instantaneous amplitude information $A(t)$ and phase information $\phi(t)$ can be extracted by multiplying Eq. (1) by $e^{-j2\pi f_0 t}$, which results in the following:

$$z_{lp}(t) = \frac{A(t)}{2} e^{j\phi(t)} + \frac{A(t)}{2} e^{-j(4\pi f_0 t + \phi(t))} \tag{2}$$

A leftward shift by $e^{-j2\pi f_0 t}$ results in moving the center frequency, f_0, to zero frequency in the spectrum of $z(t)$. If $z(t)$ in Eq. (2) is subjected to an ideal low-pass filter (LPF) with a cutoff frequency $f_c < f_0$, then the filtered signal $z_{lp}(t)$ will contain only the component of interest and the following equations can be obtained:

$$z_{lp}(t) = \frac{A(t)}{2} e^{j\phi(t)} \tag{3}$$

$$A(t) = 2|Z_{lp}(t)| \tag{4}$$

$$\phi(t) = \arctan\left(\frac{imag\left(Z_{lp}(t)\right)}{real\left(Z_{lp}(t)\right)}\right) \tag{5}$$

When a modulating frequency is not fixed as described above but varies as a function of time, the signal x(t) can be written as follows:

$$x(t) = dc(t) + A(t)\cos\left(\int_0^t 2\pi f(\tau)\, d\tau + \phi(t)\right) \tag{6}$$

Similar to the operations in Eqs. (1) and (2), multiplying Eq. (6) by $e^{-j\int_0^t 2\pi f(\tau) d\tau}$ yields both instantaneous amplitude,

$A(t)$, and instantaneous phase, $\phi(t)$, which can be described by the following equation:

$$\begin{aligned} z(t) &= x(t)\, e^{-j\int_0^t 2\pi f(\tau)d\tau} \\ &= dc(t)\, e^{-j\int_0^t 2\pi f(\tau)} + \frac{A(t)}{2} e^{j\phi(t)} \\ &\quad + \frac{A(t)}{2} e^{-j\left(\int_0^t 4\pi f(\tau)d\tau + \phi(t)\right)} \end{aligned} \tag{7}$$

From Eq. (7), if z(t) is filtered with an ideal LPF with a cutoff frequency $f_c < f_0$, then the filtered signal $z_{lp}(t)$ can be obtained with the same instantaneous amplitude A(t) and phase $\phi(t)$ as provided in Eqs. (4) and (5). The instantaneous frequency is given by:

$$f(t) = f_0 + \frac{1}{2\pi}\frac{d\phi(t)}{dt} \tag{8}$$

For variable frequencies, the center frequency, f_0, is used to estimate the instantaneous frequency within the arbitrarily set frequency band using Eq. (8).

By changing the center frequency followed by using the variable frequency approach of Eqs. (1) and (6), respectively, as well as the LPF, the signal, $x(t)$, can be decomposed into the sinusoid modulations by the complex demodulation technique, as follows:

$$\begin{aligned} x(t) &= \sum\nolimits_i d_i \\ &= dc(t) + \sum\nolimits_i A_i(t)\cos\left(\int_0^t 2\pi f_i(\tau)\, d\tau + \phi_i(t)\right) \end{aligned} \tag{9}$$

The instantaneous frequency and amplitude of d_i can be calculated using the Hilbert transform. The entire TFS can be obtained by the calculation of the Hilbert transform of Eq. (9) for all time points for the obtained lowpass-filtered frequency components, as described in Eq. (3). According to the properties of VFCDM defined in the paper [25], the frequency margin for a particular bandwidth can be calculated as follows:

$$P(BW) = \iint_{BW} |S_t(\omega)|^2\, d\omega dt = \int_{BW} |S(\omega)|^2, \tag{10}$$

where $S(\omega)$ and BW represent the TFS of the signal obtained by the CDM, and the bandwidth of the frequency range of each decomposed signal, respectively.

In summary, the VFCDM technique consists of two steps. The first step is to use complex demodulation to obtain an estimate of the TFS. In this step, a bank of LPFs is used to decompose the signal into a series of band-limited signals. The second step is to choose only the dominant frequencies of interest for further refinement of the time-frequency resolution using the VFCDM approach. Note that MA components must be removed from the TFS of PPG signals before the second step.

3) MA REMOVAL

The TFS of each accelerometer signal can be obtained using VFCDM, as described in the previous section. In Fig. 2, the TFS of a PPG signal (a) and of tri-axial accelerometer data (b-d) are shown. The frequency resolution of the TFS was set to 0.0391 Hz. The MA frequencies are distinct from the PPG signal's dominant frequencies. If the MA frequencies are not removed from the TFS of Fig. 2a, we obtain incorrect HR estimates, especially around 420-580 seconds, as shown in Fig. 3. This is because the amplitudes of the dominant frequencies associated with the accelerometer are greater

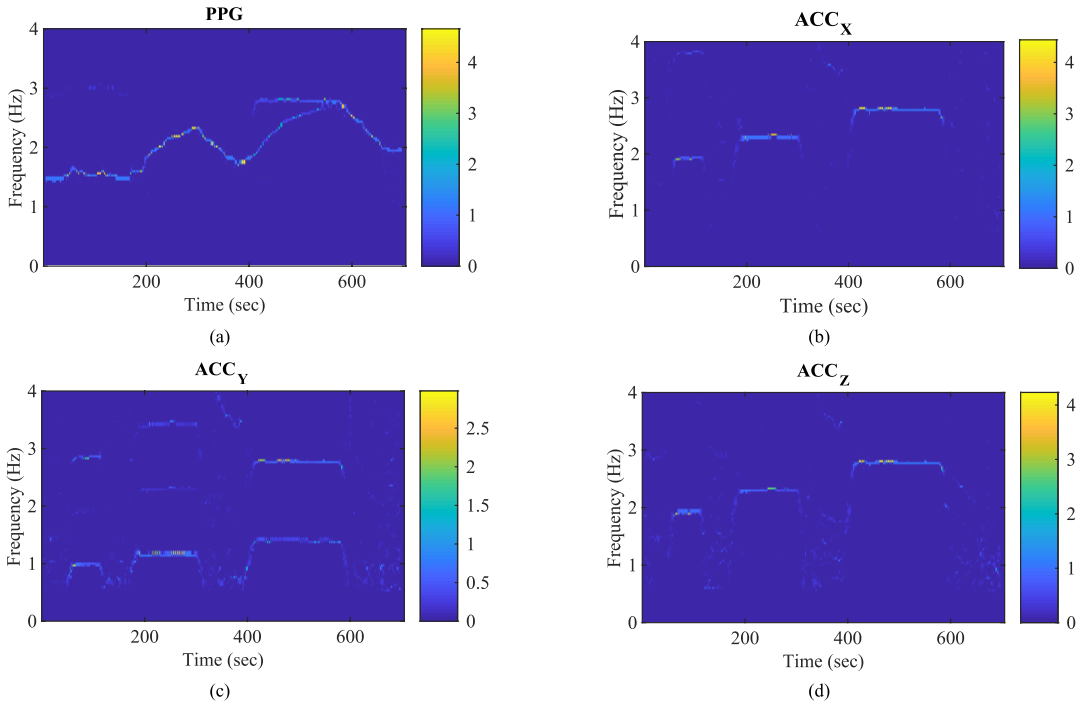

FIGURE 2. An example of the TFS of PPG and accelerometer data (subject 21).

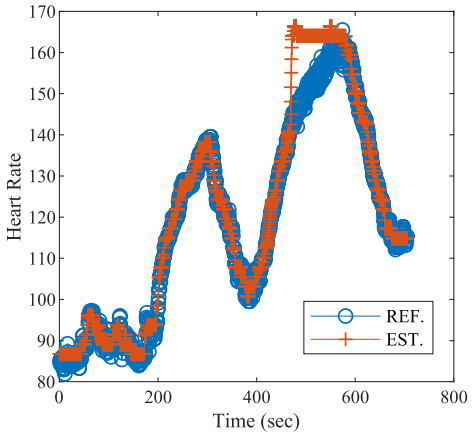

FIGURE 3. Estimated HR of Subject 21 without MA rejection.

than the heart rate at these time points, hence, the former would be selected as the chosen heart rate. Therefore, the MA-associated frequencies can be removed by subtracting the TFS of each accelerometer signal from that of the PPG signal. Note that information about the phase of the PPG and accelerometer signals is not needed for MA removal. By using the property provided in Eq. (10), the desired MA-removed TFS can be obtained as follows:

$$P_{MA-removed}(BW) = \int_{BW} \left[max\left\{0, \left|S_{ppg}(\omega)\right| - \sum\nolimits_c \left|S_{acc_c}(\omega)\right|\right\}\right]^2 c \in \{x, y, z\} \tag{11}$$

To prevent removal of true HR components from the TFS of PPG in a resting state, a threshold for the accelerometer signals was set as follows:

$$P_{seg}(BW) = \begin{cases} Eq.10, & \mu_{RMS(ACC_c)} < TH_{ACC} \\ Eq.11, & otherwise, \end{cases} \quad c \in \{x, y, z\} \tag{12}$$

where $\mu_{RMS(ACC_c)}$ represents an average of the root mean square of all accelerometer channels and TH_{ACC} is the threshold value of 0.5 for the IEEE dataset and 300 for Chon Lab dataset. The threshold values of the accelerometers were different for these two datasets because the watch sensors were made by different vendors.

Figure 4 shows an example of the MA-removed TFS of the PPG signal. By comparing with Fig. 2 (a), most of the MA frequencies are removed. As shown in Fig. 4, some of the noise artifacts (starting ~400 seconds and around 2.8 Hz) are still retained. However, for each time instant, under the condition that we retain the highest amplitude and that heart rates cannot increase more than 6 beats from the prior beat, these remnant beats will not be chosen as the detected beats.

4) POSTPROCESSING

Any remaining MA are further removed and then interpolated using polynomial regression followed by the cubic spline of

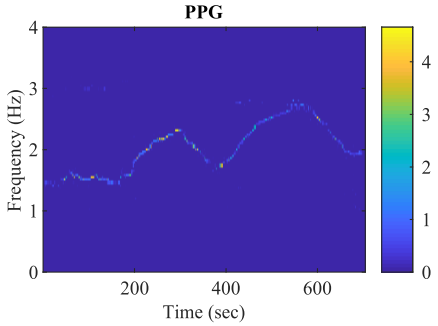

FIGURE 4. An example of denoised TFS of PPG (subject 21).

missing heart rates due to MAs. First, any abrupt HR changes (more than 6 heart beats from the previous beat) are removed. Thus, any heart rate segments shorter than a second and HRs greater than 6 beats from the previous beat are removed, as these signify abrupt changes in HRs that are due to MA. Moreover, for the first 30 seconds of the TFS via VFCDM we remove any heart rates that are more than three scaled median absolute deviations (MAD) away from the median, calculated as follows:

$$\begin{aligned} scaled\ MAD &= k \cdot median\left(\left|x_t - median\left(x\right)\right|\right) \\ k &= 1/(\Phi^{-1}(3/4)), \end{aligned} \tag{13}$$

where Φ^{-1} represents the reciprocal of the quantile function. We use the MAD criterion on the first 30 seconds of the TFS because of the distortion seen in the beginning portion of the spectrum with VFCDM.

The next step is to perform polynomial regression on each sample with estimated HRs that are 20 seconds prior to and 20 seconds after the current sample, but ignoring the outliers that are more than three scaled MAD away from the median. If differences between the estimated values by the 3rd-order regression and the sample values are larger than 6 (the maximum HR difference that we set above), the sample is rejected. Finally, the cubic spline algorithm is used to interpolate between removed samples and the retained HRs.

III. RESULTS

To evaluate the results, E_1, the average absolute error, and E_2, the average relative error, were calculated as follows:

$$E_1 = \frac{1}{N}\sum_{k=1}^{N}\left|HR_{est}(k) - HR_{ref}(k)\right| \tag{14}$$

$$E_2 = \frac{1}{N}\sum_{k=1}^{N}\frac{\left|HR_{est}(k) - HR_{ref}(k)\right|}{HR_{ref}(k)} \times 100 \tag{15}$$

where N, HR_{est}, and HR_{ref} represent the total number of HR estimates, estimated HR, and the reference HR, respectively. Eqs. (14-15) are used for both the post-processing and windowed approaches. The reference HR is calculated from the ECG signal. In Table 2, our method—consisting of the post-processing of both the entire dataset and 12-sec windowed segments—is compared with the WFPV method (Wiener

filter and phase vocoder) using the online post-processing method for both databases; the code is publicly available in Github [17]. We chose to compare our method with WFPV since it has been shown to be one of the best methods for the IEEE Signal Processing Challenge Cup dataset [27]. As shown in Table 2, our method, both the post-processing and windowed approaches, consistently outperforms WFPV for both E_1 and E_2 for all subjects in the Chon lab database. There is not much difference in E_1 and E_2 values between the post-processing and windowed approaches. Our windowed approach is a more direct comparison to WFPV since it also uses data segments. For the IEEE Cup database, both of our approaches outperform WFPV, except for subject 10, with the post-processing method. Considering both databases, the average E_1 is 2.94 ± 0.97 beats per minute and average E_2 is 2.42 ± 0.91 beats per minute with our windowed method. These values are 71% and 94% less than E_1 and E_2 for WFPV, respectively. Figure 5 shows a representative HR tracking result with the proposed windowed approach. As shown, heart rates are in good agreement with the reference values.

TABLE 2. Results.

Index	WFPV		TVSMART (12-sec window)		TVSMART (post-processing of the entire dataset)	
	E_1	E_2	E_1	E_2	E_1	E_2
IEEE Cup data						
1	2.93	2.36	2.29	1.83	2.36	1.82
2	2.78	2.44	2.48	2.40	2.26	2.01
3	2.78	2.25	2.45	1.97	1.89	1.46
4	3.76	2.90	3.34	2.55	3.15	2.44
5	4.39	3.10	4.14	2.85	4.08	2.82
6	2.70	2.13	2.34	1.81	2.29	1.76
7	2.34	1.78	2.13	1.59	2.12	1.57
8	3.38	2.74	2.71	2.19	2.61	2.08
9	2.99	2.37	2.66	2.06	2.62	2.04
10	3.90	2.43	3.81	2.37	4.72	2.92
11	3.57	2.32	3.46	2.21	3.52	2.24
12	3.72	2.60	3.46	2.35	3.30	2.27
Chon Lab Data						
13	2.15	1.84	1.51	1.25	1.38	1.15
14	9.85	9.17	4.19	3.97	4.16	4.04
15	9.80	9.61	4.60	4.29	5.10	4.55
16	3.92	3.44	2.30	2.05	2.45	2.20
17	5.25	4.94	3.26	2.99	3.30	2.98
18	18.49	22.97	4.55	3.81	4.19	3.57
19	11.29	11.92	3.89	4.28	4.01	4.32
20	6.09	6.09	2.45	1.93	2.49	1.94
21	1.89	1.61	1.24	1.03	1.25	1.01
22	2.57	2.70	1.45	1.54	1.35	1.42
Mean						
1-12	3.27	2.45	2.94	2.18	2.91	2.12
13-22	7.13	7.43	2.94	2.71	2.97	2.72
1-22	5.03	4.71	2.94	2.42	2.94	2.39
Standard Deviation						
1-12	± 0.58	± 0.34	± 3.68	± 3.79	± 0.83	± 0.43
13-22	± 4.99	± 6.17	± 4.96	± 5.91	± 1.31	± 1.28
1-22	± 3.90	± 4.85	± 4.31	± 4.90	± 1.07	± 0.97

Fig. 6a shows the Pearson correlations between the estimated and reference HRs whereas Fig. 6b shows a Bland-Altman plot with a mean difference of ±0.3, which

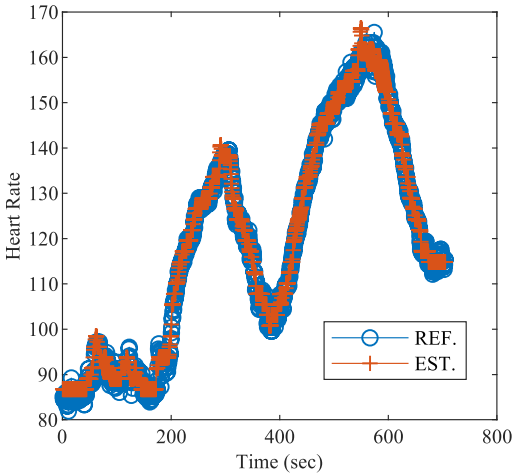

FIGURE 5. Reference and estimated HR of Subject 21.

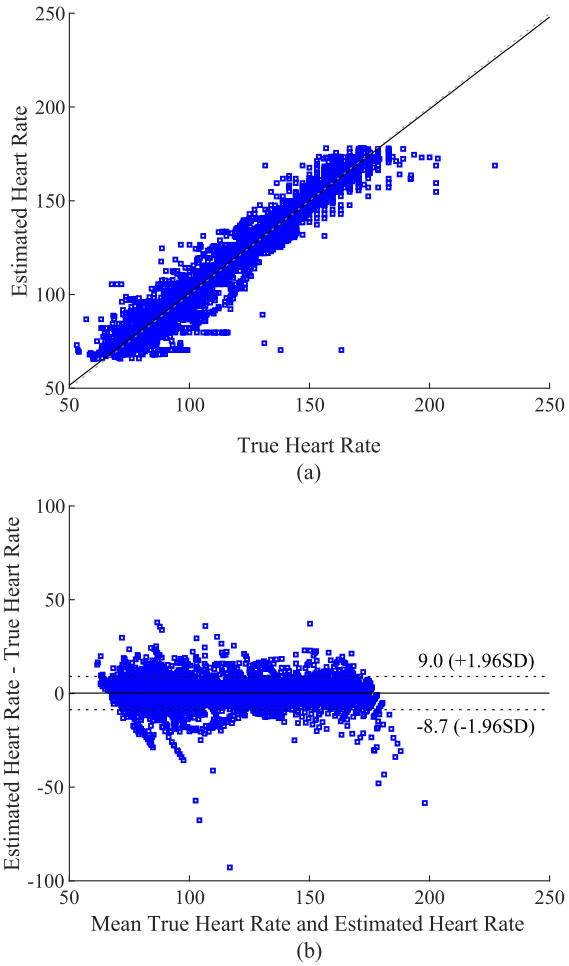

FIGURE 6. (a) Pearson correlation between the estimated HR and the reference HR (correlation coefficient = 0.98), (b) Bland-Altman plot for both IEEE signal processing challenge cup and chon lab databases.

signifies the 95% confidence limit between the estimated HR and the reference HR.

We compared the number of free parameters that are required for estimating heart rates. For this purpose, we compared our method against TROIKA, JOSS, SpaMA,

and WFPV. For our HR estimation method, the accelerometer threshold for determining MA, the LPF filter order, and the cutoff frequency for VFCDM must be preset; for our post-processing stage, the maximum HR difference and the length to obtain a spline coefficient must also be chosen. Hence, our implementation requires only three and two parameters for each stage, which is significantly fewer than other methods, as shown in Table 3. Details of the numbers of parameters required for the other methods compared are provided in [24].

TABLE 3. Number of parameters.

	TROIKA	JOSS	SpaMA	WFPV	TVSMART (Window)	TVSMART (Entire)
HR estimation	10+	5	6	2	3	2
Post-processing	10+	10+	5	4	2	2

Matlab computation times for post-processing of the entire data and a 12-sec windowed segment were 16.56 sec and 1.79 sec, respectively, using an Intel Xeon CPU running at 2.9 GHz.

We also examined the two algorithms' performance during the slow and fast exercise components of the experiment. The slow and fast labels in Table 4 refer to walking and running phases of the experiment, respectively. For both datasets, our TVSMART provides lower E_1 and E_2 errors during fast exercise than during slow exercise. The same is true for WFPV for the IEEE dataset, but the reverse is seen with the Chon Lab dataset. TVSMART resulted in a reduction of 20.8% for E_1 and 24.4% for E_2 for the slow phase, and 53.2% for E_1 and 62.9% for E_2 for the fast phase when compared to WFPV. Typically, the cyclical artifacts during running (fast phase) are easier to remove than are the less repetitive artifacts encountered during the slow walking phase of the experiment. This is reflected in our TVSMART results for both datasets but is only seen with the IEEE dataset for WFPV.

TABLE 4. Comparison of WFPV and TVSMART during slow walking and fast running phases of the experiment.

Dataset		WFPV		TVSMART (Window)	
		Slow	Fast	Slow	Fast
IEEE	E_1	4.00	3.08	3.68	2.71
	E_2	3.76	2.15	3.26	1.87
Chon Lab	E_1	5.00	8.89	3.35	2.63
	E_2	5.27	9.28	3.47	2.15
All	E_1	4.46	5.72	3.53	2.68
	E_2	4.44	5.39	3.36	2.00

IV. DISCUSSION and CONCLUSION

In this paper, we described a novel method for tracking beat-to-beat heart rates. To date, other published algorithms for HR tracking are all based on reporting an average of 8-second heart rates for each time instant. Thus, an accurate assessment of the beat-to-beat HR fluctuations cannot be made with other approaches. This is especially important and relevant during intense exercise since heart rates fluctuate significantly from one beat to the next.

Our algorithm is able to provide beat-to-beat estimates of HRs rather than an average of 8-second HR because we use a high resolution time-varying spectral density approach using the VFCDM method. Specifically, TFS of the tri-axial accelerometer signals are subtracted from the PPG signal to reject motion artifacts' frequencies. While this step removes most of the dynamics of motion artifacts that are reflected in the accelerometers, other noise and non-periodic motion artifact sources may remain. Thus, further post-processing procedures were used to remove the remaining noise and non-periodic motion artifacts using the spline regression, scaled MAD, and a cubic spline algorithm to interpolate between the missing and retained heart rates.

Our algorithm yields lower errors, albeit marginally, than does WFPV for the IEEE dataset. However, there are much more pronounced error reductions with our algorithm over WFPV for the Chon lab data. The large error reductions are most pronounced for subjects 18 and 19, but we also see similar reductions for subjects 14 and 15. Thus, we do not believe these four out of the 10 subjects' results are outliers since they represent 40% of the data.

Our error rates, calculated on a beat-to-beat basis, are, as expected, slightly higher than those of other published methods such as TROIKA, JOSS, SpaMA, and WFPV (not shown but provided in the references) since these methods reported results based on 8-sec averaged heart rates, which smooth out fluctuations in heart rates. In particular, the error rates based on 8-sec segment's averaged heart beats of our algorithm is 24.96 % and 27.02 % higher for E_1 and E_2, respectively, when compared to WFPV's approach with the IEEE Signal Processing Challenge Cup dataset. However, for the Chon lab dataset, our algorithm performed better, as WFPV fared poorly on this data. Our algorithm's error rates were lower by 83.55% and 73.85% for E_1 and E_2, respectively, on an 8 second segment's averaged heart rates. In addition, when we calculated the error rates using beat-to-beat HR estimates for both WFPV and our algorithm, we found that E_1 was lower by 71% and E_2 was 94% lower with our method for the two combined datasets. As WFPV was shown to provide better results than TROIKA, JOSS, and SpaMA, we can conjecture that, for beat-to-beat HR estimation, our approach will also outperform these methods. Note that we chose to compare our method only to WFPV since this algorithm is publicly available and its performance is better than most of the published algorithms to date.

In addition to heart rate tracking, our approach will be most useful to accurately detect heart rates for subjects with arrhythmias—in particular, fast ventricular atrial fibrillation and premature atrial contraction with fast heart rates. In these cases, the heart rates vacillate rather suddenly [28]. Most algorithms which provide 8-sec averaging of heart rates will miss these events, whereas our method has the capability to track these sudden increases or decreases in heart rates.

Also note that our method is computationally efficient and it requires only a few parameters that need to be

set *a priori*. Other published algorithms are generally complex and require many free parameters that need to be adjusted.

In summary, our method provides for the first time a means to estimate beat-to-beat heart rates rather than 8 second segment averaged heart beats for each time instant, which masks highly varying heart rate dynamics especially during intense exercise. The proposed algorithm is especially applicable for estimating heart rates during high intensity exercise and during the types of arrhythmias which lead to significant changes in heart rates from one beat to the next.

REFERENCES

[1] D. Castaneda, A. Esparza, M. Ghamari, C. Soltanpur, and H. Nazeran, "A review on wearable photoplethysmography sensors and their potential future applications in health care," *Int. J. Biosensors Bioelectron.*, vol. 4, no. 4, pp. 195–202, 2018.

[2] K. K. F. Tsoi, J. Y. H. Wong, M. P. F. Wong, G. K. S. Leung, B. K. K. Bat, F. C. H. Chan, Y.-H. Kuo, H. H. M. Lo, and H. M. L. Meng, "Personal wearable devices to measure heart rate variability: A framework of cloud platform for public health research," in *Proc. Int. Conf. Digit. Health*, 2017, pp. 207–208.

[3] E. E. Dooley, N. M. Golaszewski, and J. B. Bartholomew, "Estimating accuracy at exercise intensities: A comparative study of self-monitoring heart rate and physical activity wearable devices," *JMIR MHealth UHealth*, vol. 5, no. 3, P. e34. Mar. 2017.

[4] M. Weenk, "Continuous monitoring of vital signs using wearable devices on the general ward: Pilot study," *JMIR MHealth Uhealth*, vol. 5, no. 7, P. e91, Jul. 2017.

[5] X. Fafoutis, B. Janko, E. Mellios, G. Hilton R. S. Sherratt, R. Piechocki, and I. Craddock, "SPW-1: A low-maintenance wearable activity tracker for residential monitoring and healthcare applications," in *eHealth 360°: International Summit on eHealth, Budapest, Hungary, June 14–16, 2016, Revised Selected Papers* (Lecture Notes of the Institute for Computer Sciences, Social Informatics and Telecommunications Engineering), vol. 181. Springer, 2017, pp. 294–305. [Online]. Available: https://link.springer.com/chapter/10.1007/978-3-319-49655-9_37

[6] D. Gregori, C. Minto, C. Lanera, and G. Lorenzoni, "Feasibility and reliability of wearable devices in measuring caloric intake: Results from a pilot study," *FASEB J.*, vol. 31, no. 1, p. 302, Apr. 2017.

[7] D. T. Weiler, S. O. Villajuan, L. Edkins, S. Cleary, and J. J. Saleem, "Wearable heart rate monitor technology accuracy in research: A comparative study between PPG and ECG technology," *Proc. Hum. Factors Ergonom. Soc. Annu. Meeting*, vol. 61, no. 1, pp. 1292–1296, Sep. 2017.

[8] K. H. Chon, S. Dash, and K. Ju, "Estimation of respiratory rate from photoplethysmogram data using time-frequency spectral estimation," *IEEE Trans. Biomed. Eng.*, vol. 56, no. 8, pp. 2054–2063, Aug. 2009.

[9] S. Lu, H. Zhao, K. Ju, K. Shin, M. Lee, K. Shelley, and K. H. Chon, "Can photoplethysmography variability serve as an alternative approach to obtain heart rate variability information?" *J. Clin. Monit. Comput.*, vol. 22, no. 1, pp. 23–29, Feb. 2008.

[10] K. H. Shelley, "Photoplethysmography: Beyond the calculation of arterial oxygen saturation and heart rate," *Anesthesia Analgesia*, vol. 105, no. 6, pp. S31–S36, Dec. 2007.

[11] G. Yoon, J. Y. Lee, K. J. Jeon, K.-K. Park, H. S. Yeo, H. T. Hwang, H. S. Kim, and I.-D. Hwang, "Multiple diagnosis based on photoplethysmography: Hematocrit, SpO_2, pulse, and respiration," *Proc. SPIE*, vol. 4916, pp. 185–189, Sep. 2002.

[12] D. U. Uguz, B. Venema, S. Leonhardt, and D. Teichmann, "Multifunctional photoplethysmography sensor design for respiratory and cardiovascular diagnosis," in *Proc. World Congr. Med. Phys. Biomed. Eng.*, 2019, pp. 905–909.

[13] J. Lee, B. A. Reyes, D. D. McManus, O. Mathias, and K. H. Chon, "Atrial fibrillation detection using an iPhone 4S," *IEEE Trans. Biomed. Eng.*, vol. 60, no. 1, pp. 203–206, Jan. 2013.

[14] K. H. Chon and D. D. McManus, "Detection of atrial fibrillation using a smartwatch," *Nature Rev. Cardiol.*, vol. 15, no. 11, pp. 657–658, 2018.

[15] G. H. Tison, J. M. Sanchez, B. Ballinger, A. Singh, J. E. Olgin, M. J. Pletcher, E. Vittinghoff, E. S. Lee, S. M. Fan, and R. A. Gladstone, C. Mikell, N. Sohoni, J. Hsieh, and G. M. Marcus, "Passive detection of atrial fibrillation using a commercially available smartwatch," *JAMA Cardiol.*, vol. 3, no. 5, pp. 409–416, 2018.

[16] M. R. Ram, K. V. Madhav, E. H. Krishna, N. R. Komalla, and K. A. Reddy, "A novel approach for motion artifact reduction in PPG signals based on AS-LMS adaptive filter," *IEEE Trans. Instrum. Meas.*, vol. 61, no. 5, pp. 1445–1457, May 2012.

[17] A. Temko, "Estimation of heart rate from photoplethysmography during physical exercise using Wiener filtering and the phase vocoder," in *Proc. 37th Annu. Int. Conf. IEEE Eng. Med. Biol. Soc. (EMBC)*, Aug. 2015, pp. 1500–1503.

[18] R. Krishnan, B. Natarajan, and S. Warren, "Motion artifact reduction in photopleythysmography using magnitude-based frequency domain independent component analysis," in *Proc. 17th Int. Conf. Comput. Commun. Netw.*, Aug. 2008, pp. 1–5.

[19] B. Pang, M. Liu, X. Zhang, P. Li, and H. Chen, "A novel approach framework based on statistics for reconstruction and heartrate estimation from PPG with heavy motion artifacts," *Sci. China Inf. Sci.*, vol. 61, no. 2, Nov. 2017, Art. no. 022312.

[20] S. Seyedtabaii and L. Seyedtabaii, "Kalman filter based adaptive reduction of motion artifact from photoplethysmographic signal," *World Acad. Sci., Eng. Technol.*, vol. 37, pp. 173–176, Feb. 2008.

[21] Z. Zhang, Z. Pi, and B. Liu, "TROIKA: A general framework for heart rate monitoring using wrist-type photoplethysmographic signals during intensive physical exercise," *IEEE Trans. Biomed. Eng.*, vol. 62, no. 2, pp. 522–531, Feb. 2015.

[22] Z. Zhang, "Photoplethysmography-based heart rate monitoring in physical activities via joint sparse spectrum reconstruction," *IEEE Trans. Biomed. Eng.*, vol. 62, no. 8, pp. 1902–1910, Aug. 2015.

[23] S. M. A. Salehizadeh, D. Dao, J. Bolkhovsky, C. Cho, Y. Mendelson, and K. H. Chon, "A novel time-varying spectral filtering algorithm for reconstruction of motion artifact corrupted heart rate signals during intense physical activities using a wearable photoplethysmogram sensor," *Sensors*, vol. 16, no. 1, p. 10, 2015.

[24] A. Temko, "Accurate heart rate monitoring during physical exercises using PPG," *IEEE Trans. Biomed. Eng.*, vol. 64, no. 9, pp. 2016–2024, Sep. 2017.

[25] H. Wang, K. Siu, K. Ju, and K. H. Chon, "A high resolution approach to estimating time-frequency spectra and their amplitudes," *Ann. Biomed. Eng.*, vol. 34, no. 2, pp. 326–338, Feb. 2006.

[26] *IEEE SP Cup IEEE Signal Processing Society*. Accessed: Nov. 11, 2018. [Online]. Available: http://archive.signalprocessingsociety.org/community/sp-cup/ieee-sp-cup-2015/.

[27] *IEEE Signal Processing Cup Heart Rate Monitoring During Physical Exercise Using Wrist-Type Photoplethysmographic (PPG) Signals*. Accessed: Jan. 31. 2019. [Online]. Available: https://sites.google.com/site/researchbyzhang/ieeespcup2015

[28] S. K. Bashar, D. Han, S. Hajeb-Mohammadalipour, E. Ding, C. Whitcomb, D. D. McManus, and K. H. Chon, "Atrial fibrillation detection from wrist photoplethysmography signals using smartwatches," *Sci. Rep.*, vol. 9, no. 1, pp. 1–10, Oct. 2019.

YOUNGSUN KONG received the B.S. and M.S. degrees in computer science and engineering from Soonchunhyang University, Asan, South Korea. He is currently pursuing the Ph.D. degree with the University Connecticut, Storrs, CT, USA.

KI H. CHON received the B.S. degree in electrical engineering from the University of Connecticut, Storrs, CT, USA, the M.S. degree in biomedical engineering from the University of Iowa, Iowa City, and the M.S. degree in electrical engineering and the Ph.D. degree in biomedical engineering from the University of Southern California, Los Angeles. He is currently the John and Donna Krenicki Chair Professor and the Head of the biomedical engineering with the University of Connecticut. He is a Fellow of the American Institute of Medical and Biological Engineering and the International Academy of Medical and Biological Engineering. He has chaired many international conferences, including his role as the Program Co-Chair for the IEEE EMBS Conference in NYC, in 2006, and as the Conference Chair for the 6th International Workshop on Biosignal Interpretation in New Haven, CT, USA, in 2009. He was an Associate Editor of the IEEE TRANSACTIONS ON BIOMEDICAL ENGINEERING, from 2007 to 2013.